

# Low-temperature synthetic route based on the amorphous nature of giant species for preparation of lower valence oxides

Kazuo Eda\*, Fumiko Kunotani, Noriki Uchiyama

*Department of Chemistry, Faculty of Science, Kobe University, Nada-ku, Kobe-shi, Hyogo-ken 657-8501, Japan*

Received 6 October 2004; received in revised form 25 February 2005; accepted 27 February 2005

Available online 19 March 2005

## Abstract

We examined low-temperature synthetic route based on the amorphous nature of giant species to succeed to prepare Cs blue bronze ( $\text{Cs}_{0.3}\text{MoO}_3$ ), which has never obtained by usual high-temperature methods, at ca. 680 K. Solid solutions ( $\text{K}_{1-x}\text{Rb}_x$ ) $_{0.28}\text{MoO}_3$  and ( $\text{Li}_{1-x}\text{Na}_x$ ) $_{0.9}\text{Mo}_6\text{O}_{17}$  were also obtained at lower temperatures (ca. 670 K). For the latter system consisting of non-isostructural end members,  $\text{Li}_{0.9}\text{Mo}_6\text{O}_{17}$ -structure type solid solution was formed even when  $0.25 < x < 0.70$ , unlike the case by the usual high-temperature methods. Metastable mixed oxides  $\text{Ln}_2\text{Mo}_3\text{O}_9$  ( $\text{Ln} = \text{La}, \text{Gd}$ ) were obtained, but not as single phases.

© 2005 Elsevier Inc. All rights reserved.

**Keywords:** Low-temperature synthesis; Blue bronze; Purple bronze; Solid solution; Lower valence oxide;  $\text{Ln}_2\text{Mo}_3\text{O}_9$

## 1. Introduction

Complex inorganic solids are generally synthesized by repeated grinding and firing of the reactant mixtures. The higher firing temperature is of essence of overcoming the diffusional limitations encountered in these syntheses. Such a higher-temperature procedure causes sometimes disadvantages as large particle size of products, inaccessibility of metastable phases, which have interesting structures and properties. This recognition has stimulated solid-state chemists to develop new synthetic techniques at lower reaction temperatures, as sol-gel processing [1–4].

Sol-gel approaches have been investigated extensively to succeed in obtaining a number of metal oxides such as  $\text{Al}_2\text{O}_3$ ,  $\text{Nb}_2\text{O}_5$ ,  $\text{MoO}_3$ ,  $\text{WO}_3$ , as well as mixed-metal oxides at lower temperatures [5]. Although the higher valence oxides have been readily obtained by these sol-gel methods, little was known about obtaining lower valence oxides. Manthirm's group and our group have

independently proposed some low-temperature synthetic routes for lower valence oxides, in which methods non-stoichiometric single-phase compounds were used as starting materials: in the case of Manthirm's group, amorphous precipitates obtained by reducing aqueous oxometalate species with  $\text{NaBH}_4$  or  $\text{KBH}_4$  [6,7] and in our case, intercalation compounds [8,9]. In these methods, unfortunately, compositional control of the single-phase compounds was difficult, because their compositions depend on various parameters such as temperature, solution pH, reactant concentrations, the nature of intermediates, etc. Thus, products usually contained some by-products.

Recently, we proposed a new low-temperature synthetic route of lower valence oxides, which route is based on the amorphous nature of giant species [10]. Fig. 1 gives a conceptual figure of this route. As the giant species we use nanosized polyoxomolybdate ions, existence of which was revealed by Müller et al. [11]. Because of difficulties of positioning extremely large species into a highly ordered lattice, the solution containing such species provides amorphous solids after drying. Because the resultant solids are mixtures in

\*Corresponding author. Fax: +81 78 503 5677.

E-mail address: [eda@kobe-u.ac.jp](mailto:eda@kobe-u.ac.jp) (K. Eda).

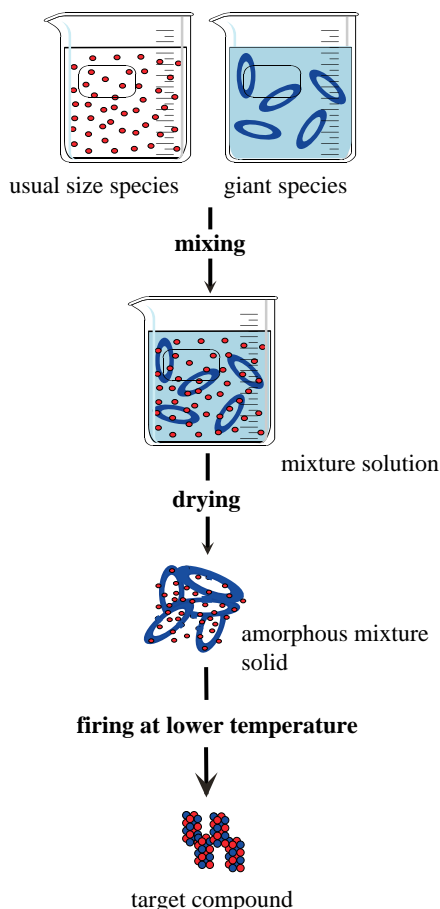


Fig. 1. Conceptual figure of low-temperature synthetic route based on amorphous nature of giant species.

atomic or molecular level and have compositional homogeneity like the mixture solution, by heat-treatment of the mixtures target compounds were formed without being constrained by the interparticle diffusional limitations encountered in the usual high-temperature methods and therefore at lower temperatures than by usual (high-temperature) methods. Furthermore, in this route compositional adjustment of the mixtures is very easily achieved only by mixing solutions in proper molar ratio. Thus, we can obtain compositionally well-adjusted products (target compounds) at low temperatures.

In the present work, we examined performance of this route using following subjects. Previously we revealed the existence of Cs blue bronze ( $\text{Cs}_{0.3}\text{MoO}_3$ ), which had been ever thought not to exist [12], using the low-temperature synthetic method based on intercalation compounds [13]. The previous method, however, had a limited range of compositional adjustment and could not provide the single-phase bronze. The present method enabled not only a synthesis at low temperature comparable to that of the previous one, but also much wider range of compositional adjustment. Therefore, firstly, we tried to prepare the single-phase bronze

throughout the present route. Furthermore, arrangement of a complicated composition was so easy that the route was expected to be very useful for preparation of the multi-components systems such as solid solutions. So, secondly, we tried to prepare  $\text{K}_{0.3-x}\text{Rb}_x\text{MoO}_3$  and  $\text{Li}_{0.9-x}\text{Na}_x\text{Mo}_6\text{O}_{17}$ , which have attracted many researchers because of their interesting properties owing to CDW or low-dimensional electronic structure [14–18]. Thirdly, we tried to prepare compounds other than alkali-metal molybdenum bronzes using the present route. Here we will present the details of the preparations of the compounds mentioned above.

## 2. Experimental

### 2.1. Preparation of GC solution

Aqueous molybdic acid was prepared by treating aqueous sodium molybdate with an ion-exchange resin (Dow Chemical Co. DowEX 50W-X8). The solution was once spray-dried into soluble amorphous powder. Then, by dissolving the powder in water, the acid solution with desired concentration (typically  $[\text{Mo}] = 0.165 \text{ M}$ ) was prepared. The solution was reduced with  $\text{H}_2/\text{Pd}$  treatment to prepare lower valence molybdic acid solution containing the molybdenum giant cluster species (GC solution). The presence of the giant species in the solution was confirmed by UV–Vis and Raman spectroscopies [19]. Mean oxidation state of Mo (MOSMo) of GC solution was controlled by reduction time. Possible maximum MOSMo value was ca. 4.5.

### 2.2. Adjustments of chemical compositions

MOSMo of GC solution was measured by cerimetric titration, and was adjusted to match that of target material by mixing with the original higher valence molybdic acid solution or by additional reduction with the  $\text{H}_2/\text{Pd}$  treatment. In order to match the chemical compositions of intermediate amorphous mixtures to those of target products, stoichiometric amounts of solutions containing desired metal cations were added to the GC solution with a proper MOSMo value. Total volume of metal-cation source solutions added was sized into one-tenth volume of the GC solution to avoid excess reduction in Mo concentration of the resulting mixture solution, if possible. As metal-cation sources carbonate or acetate salts were used in the present work.

### 2.3. Preparation and heat-treatment of amorphous mixtures

Amorphous mixtures were obtained by drying the composition-adjusted mixture solutions in vacuo.

Heat-treatments of the amorphous mixtures were carried out at a heating rate of 10 K/min usually on a TG-DTA equipment, and in a tube furnace when a larger amount of product was needed.

#### 2.4. Measurements

Powder X-ray diffraction (XRD) patterns of the samples were measured using a Bruker AXS MXP3VZ X-ray diffractometer with  $\text{CuK}\alpha$  radiation. Rietveld analysis of the diffraction pattern was performed using Rietan 2000 [20]. The compositions of the products were analyzed by a HITACHI 180-80 atomic absorption spectrometer and by the method of Choain and Marion [21]. Infrared spectra were measured using a Perkin-Elmer Spectrum 2000 FT-IR spectrometer. A Bruker AXS TG-DTA 2010 system was applied to TG-DTA analysis.

### 3. Results and discussion

#### 3.1. Preparation of cesium blue bronze

In order to determine a condition suitable for preparation of single-phase Cs blue bronze, we prepared the intermediate mixtures with Cs content ( $[\text{Cs}]/[\text{Mo}]$ ) ranging from 0.25 to 0.35 and MOSMo values ranging from 5.75 to 5.67, using our synthetic route. The mixtures were all successfully prepared as amorphous solids. By heating them at 683 K in  $\text{N}_2$ , various crystalline phases were obtained depending on Cs content and/or MOSMo value. Fig. 2 gives the XRD patterns of the heat-treated (at 683 K in  $\text{N}_2$ ) products. At Cs content of 0.25 (MOSMo = 5.75) a mixture of hexagonal Cs bronze ( $\text{Cs}_{0.14}\text{MoO}_3$ ) [22] and an undefined compound was obtained. Cs blue bronze was formed in the range of Cs content from 0.26 to 0.30. Single phase of the bronze was obtained at Cs content of 0.28. For Cs content exceeding 0.3 the formation of Cs red bronze ( $\text{Cs}_{0.33}\text{MoO}_3$ ) occurred.

The nature of the heat-treated product with Cs content of 0.28 was investigated in detail. Atomic absorption and redox titration analyses confirmed the composition of the product as  $\text{Cs}_{0.28}\text{MoO}_3$ : calculated Cs 20.5 wt%, Mo 53.0 wt%, MOSMo 5.72; found Cs 20.0 wt%, Mo 52.1 wt%, MOSMo 5.72. The XRD pattern of the product, which was precisely measured in the  $2\theta$  range from  $8^\circ$  to  $120^\circ$  with a step scan mode ( $0.02^\circ$  of step size and 10 s of count time per step), agreed well with the pattern simulated using the atomic parameters of isomorphous  $\text{K}_{0.28}\text{MoO}_3$  [23] (replace  $\text{K}^+$  to  $\text{Cs}^+$ ) and the lattice constants of Cs blue bronze determined previously [13]. Fig. 3 shows the results of Rietveld analysis of the XRD pattern. Table 1 lists atomic parameters. The (monoclinic) lattice constants refined

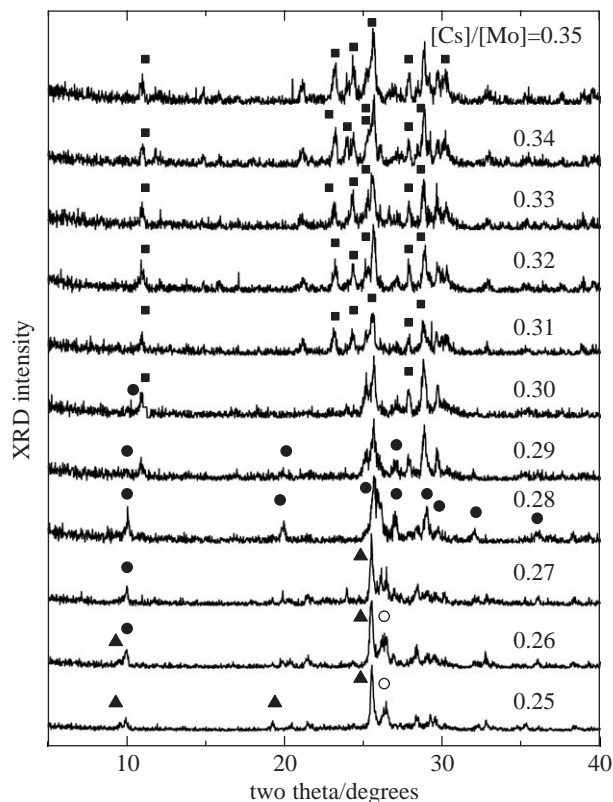


Fig. 2. XRD patterns of the heat-treated (at 683 K in  $\text{N}_2$ ) products. Symbols ▲, ○, ●, and ■ indicate hexagonal Cs bronze, undefined phase, Cs blue bronze, and Cs red bronze, respectively.

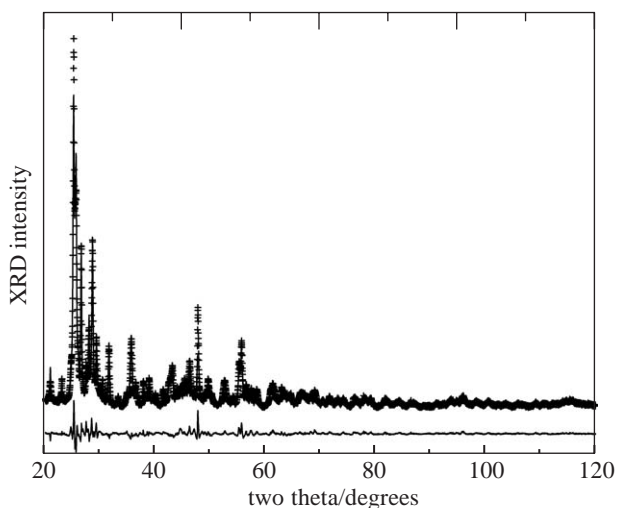


Fig. 3. The final Rietveld refinement plot for  $\text{Cs}_{0.28}\text{MoO}_3$ . Continuous line corresponds to observed pattern, the small crosses (+) the calculated values. The bottom trace depicts the differential plot of experimental and calculated intensities.

were  $a = 19.391(2) \text{ \AA}$ ,  $b = 7.559(1) \text{ \AA}$ ,  $c = 10.524(1) \text{ \AA}$ ,  $\beta = 121.33(1)^\circ$ , and  $V = 1317.6(2) \text{ \AA}^3$ , respectively. The space group was  $C_2/m$  (No. 12). The agreement factors were  $R_{\text{wp}} = 13.49\%$  and  $R_p = 10.60\%$ , respectively, with

Table 1  
Atomic parameters for  $\text{Cs}_{0.28}\text{MoO}_3$

Atom	Site	$x$	$y$	$z$	Occupancy	$B$ ( $\text{\AA}^2$ )
Mo1	4i	0.2207(6)	0	0.1839(9)	1	0.26
Mo2	8j	0.4263(4)	0.2554(12)	0.0405(7)	1	1.60
Mo3	8j	0.1450(4)	0.2534(10)	0.3393(7)	1	0.78
O1	4	1/4	1/4	1/2	1	0.10
O2	4i	0.245(3)	0	0.050(7)	1	0.12
O3	4i	0.332(3)	0	0.367(6)	1	0.12
O4	4i	0.437(3)	0	0.021(7)	1	0.12
O5	4i	0.887(3)	0	-0.050(6)	1	0.25
O6	4i	0.181(3)	0	0.328(7)	1	2.92
O7	4i	0.670(3)	0	0.246(7)	1	0.45
O8	8j	0.410(2)	0.216(7)	0.180(5)	1	2.85
O9	8j	0.172(2)	0.269(6)	0.182(3)	1	0.12
O10	8j	0.085(2)	0.219(6)	0.417(3)	1	0.13
O11	8j	0.042(2)	0.255(8)	0.146(4)	1	0.11
Cs1	2d	0	1/2	1/2	0.80 <sup>a</sup>	1.81
Cs2	4i	0.8204(4)	0	0.2710(9)	1.00 <sup>a</sup>	1.97

<sup>a</sup>Occupancies of Cs1 and Cs2 were fixed so as to match the composition  $\text{Cs}_{0.28}\text{MoO}_3$ .

the goodness-of-fit  $S = 3.52$ , indicating fairly good fit. According to these results, it can be noted that the present synthesis route is very useful to prepare Cs blue bronze, which has never obtained by usual high-temperature methods.

#### 4. Preparation of multi-component systems such as solid solutions

##### 4.1. Binary system between K and Rb blue bronzes

According to the present investigation, the alkali-metal content ( $[\text{M}]/[\text{Mo}]$ ,  $M = \text{K}, \text{Rb}$ ) and the MOSMo value suitable for preparation of single-phase K and Rb blue bronzes ( $\text{M}_{0.3}\text{MoO}_3$ ) were 0.28 and 5.72, respectively. In order to obtain solid solutions between K and Rb blue bronzes, some amorphous mixtures with alkali-metal content ( $([\text{K}] + [\text{Rb}])/[\text{Mo}] = 0.28$  and  $\text{MOSMo} = 5.72$ ) were prepared using our synthetic route. Atomic absorption and redox titration analyses confirmed compositions of their heat-treated (at 673 K in  $\text{N}_2$ ) products as  $(\text{K}_{1-x}\text{Rb}_x)_{0.28}\text{MoO}_3$ . Table 2 gives analyzed alkali-metal contents of the products (named K–Rb  $n$ ,  $n = 1-5$ , in ascending order for the Rb content). Fig. 4 shows XRD patterns of the products. Peaks of each product were indexed as a single phase and indicated that all the products had the structure of blue bronze. Because of changes in lattice parameters depending on Rb fraction  $x$  of the sample, fairly large shifts of peak positions were observed. Fig. 5 shows the plots of the lattice parameters  $a$ ,  $b$ ,  $c$ ,  $\beta$ , and  $V$  vs. Rb fraction  $x$ . The lattice parameters increase monotonously with  $x$ , indicating the formation of continuous

Table 2  
Alkali-metal contents of heat-treated products obtained for the K–Rb system

Sample	$[\text{K}]/[\text{Mo}]$	$[\text{Rb}]/[\text{Mo}]$	Rb fraction $x$
K–Rb 1	0.28	0.00	0.0
K–Rb 2	0.20	0.08	0.29
K–Rb 3	0.13	0.15	0.54
K–Rb 4	0.06	0.22	0.79
K–Rb 5	0.00	0.28	1.0

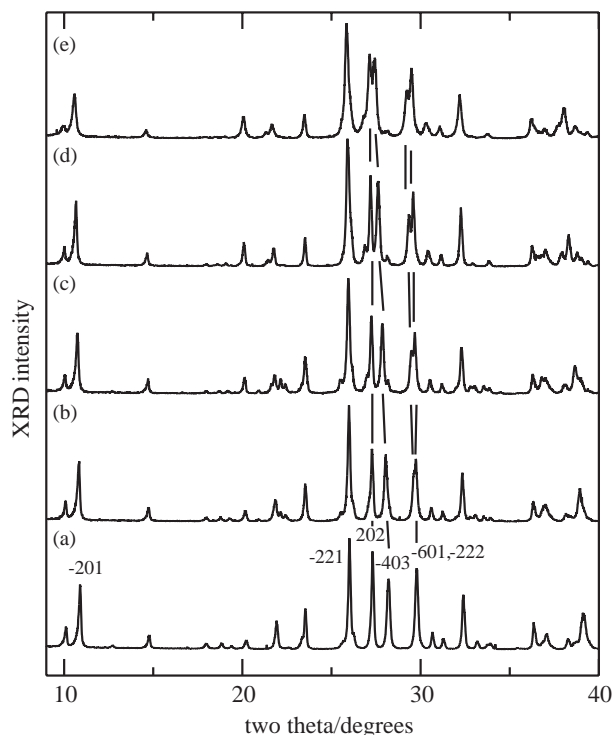


Fig. 4. XRD patterns of the products  $(\text{K}_{1-x}\text{Rb}_x)_{0.28}\text{MoO}_3$ :  $x = 0.0$  (a), 0.29 (b), 0.54 (c), 0.79 (d), and 1.0 (e). Some short lines linking related peaks specify the shifts of peak positions.

solid solutions between  $\text{K}_{0.28}\text{MoO}_3$  and  $\text{Rb}_{0.28}\text{MoO}_3$ . IR spectra of all the products showed absorption bands at the same frequencies 954, 942, 909, 644, and  $516 \text{ cm}^{-1}$  in the range  $1200-500 \text{ cm}^{-1}$  and indicated that there were no large differences in the Mo–O frameworks of the products regardless of changes in  $x$  of the sample. The above results imply that the present synthesis route is very useful to prepare solid solutions between the blue bronzes at lower temperatures.

##### 4.2. Binary system between Na and Li purple bronzes

According to a preliminary investigation, alkali-metal content ( $[\text{M}]/[\text{Mo}]$ ,  $M = \text{Li}, \text{Na}$ ) and MOSMo value, which were suitable for preparation of single phases of Li and Na purple bronzes, were 0.16 and 5.50,

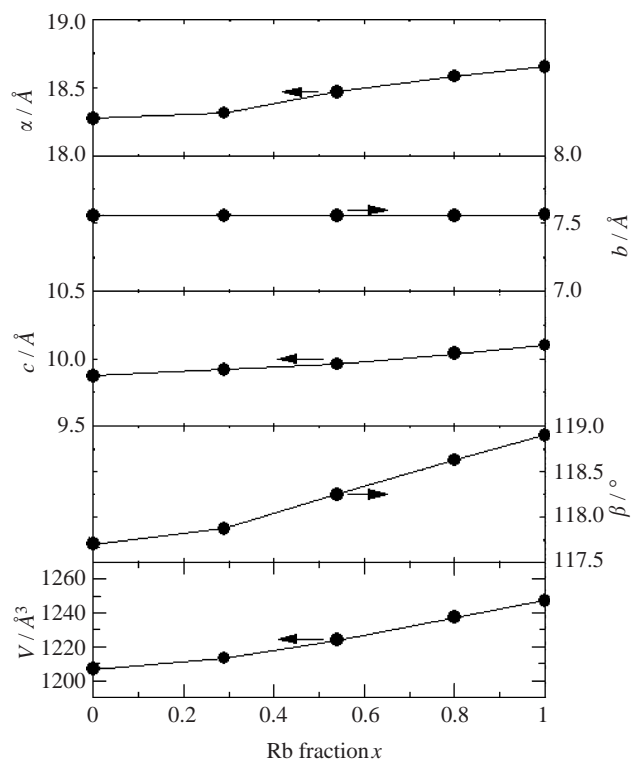


Fig. 5. Plots of lattice parameters  $a$ ,  $b$ ,  $c$ ,  $\beta$ , and  $V$  vs. Rb fraction  $x$  for  $(K_{1-x}Rb_x)_{0.28}MoO_3$ .

Table 3  
Alkali-metal contents of heat-treated products obtained for the Li–Na system

Sample	[Li]/[Mo]	[Na]/[Mo]	Na fraction $x$
Li–Na 1	0.16	0.00	0.0
Li–Na 2	0.11	0.05	0.31
Li–Na 3	0.07	0.09	0.56
Li–Na 4	0.05	0.11	0.69
Li–Na 5	0.00	0.17	1.0

respectively. Through the same procedure described above we obtained mixed compounds between Li and Na purple bronzes ( $(Li_{1-x}Na_x)_{0.9}Mo_6O_{17}$ ). Table 3 gives analyzed alkali-metal contents of the products (named Li–Na  $n$ ,  $n = 1–5$ , in ascending order for the Na content). Fig. 6 shows XRD patterns of the heat-treated products. Peaks of each product are indexed as a single phase. In contrast with the case of K and Rb blue bronzes, there are only subtle shifts of peak positions in the present case. To understand the data correctly it should be mentioned that Li and Na purple bronzes are not isostructural with each other [24,25], although both the bronzes give quite similar diffraction patterns. One of their main structural discrepancies is that Na purple bronze has a regular  $ReO_3$  type Mo–O framework as one of the structural constitution units, while Li purple

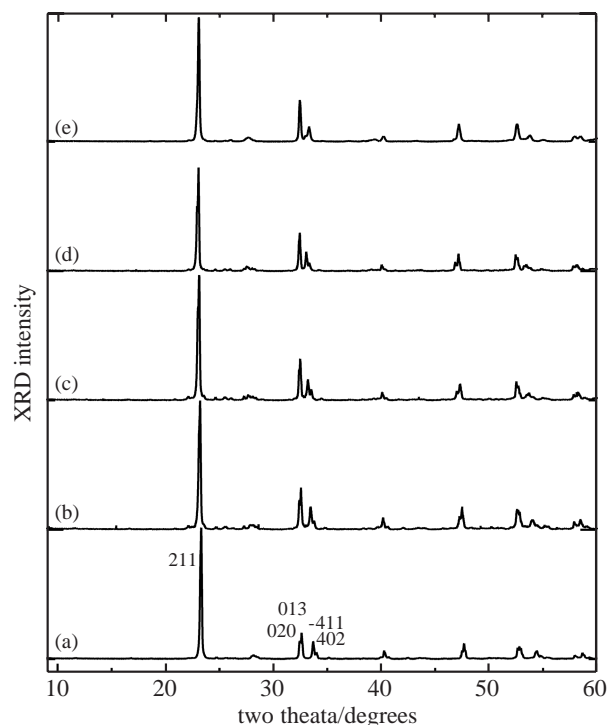


Fig. 6. XRD patterns of the products  $(Li_{1-x}Na_x)_{0.9}Mo_6O_{17}$ :  $x = 0.0$  (a), 0.31 (b), 0.56 (c), 0.69 (d), and 1.0 (e).

bronze has a distorted  $ReO_3$  type Mo–O framework. Fig. 7 shows plots of the lattice parameters  $a$ ,  $b$ ,  $c$ ,  $\beta$ , and  $V$  vs. Na fraction  $x$  of sample. In the present case, the lattice parameters deviated from a simple linear dependence on the fraction  $x$  of Na having a larger cationic radius than Li. Especially parameters  $c$  and  $V$  have maximum values at around  $x = 0.70$ , while the parameter  $\beta$  is almost constant and equal to the value of Li purple bronze in the  $x$  range from 0.0 to 0.70. These results imply that  $Li_{0.9}Mo_6O_{17}$  type solid solutions are formed in the range. IR spectra of the products given in Fig. 8 supported this.  $Li_{0.9}Mo_6O_{17}$  bronze has a characteristic spectral structure in the frequency range  $900–700\text{ cm}^{-1}$ , which is not observed for  $Na_{0.9}Mo_6O_{17}$ . The products with  $x < 0.70$  exhibit similar spectral structure, supporting that they have  $Li_{0.9}Mo_6O_{17}$  type structure. According to the literature [26],  $(Li_{1-x}Na_x)_{0.9}Mo_6O_{17}$  obtained by the high-temperature method shows a lattice constants vs.  $x$  dependence different from the present case. For comparison the results obtained on the compounds prepared by the high-temperature method were also given in Fig. 7. Apparent discrepancies were observed in the range  $0.25 < x < 0.70$  between the compounds prepared by different synthetic works, suggesting that  $Li_{0.9}Mo_6O_{17}$  type solid solution with  $0.25 < x < 0.70$  was formed by the present synthetic route, not by usual high-temperature synthetic methods.

The above results indicate that our synthetic route provides not only an easy preparation method of binary

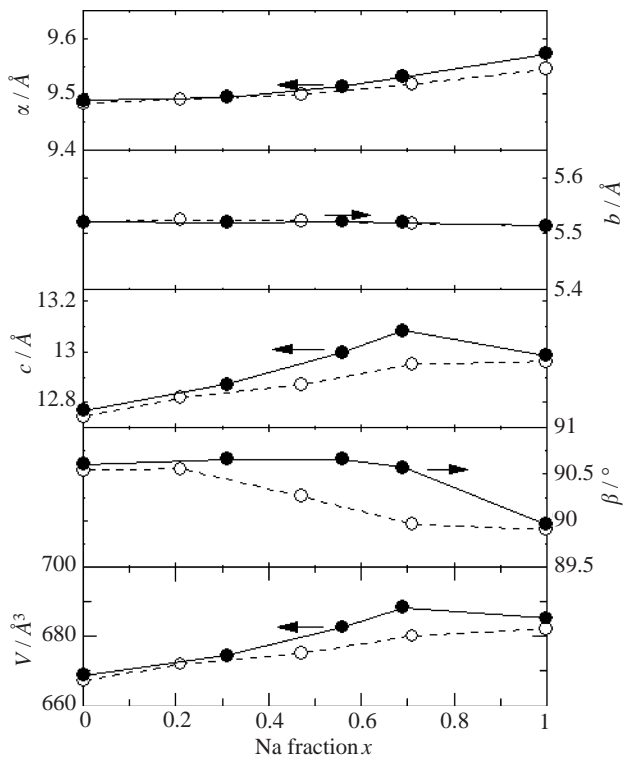


Fig. 7. Plots of lattice parameters  $a$ ,  $b$ ,  $c$ ,  $\beta$ , and  $V$  vs. Na fraction  $x$  for  $(\text{Li}_{1-x}\text{Na}_x)_{0.9}\text{Mo}_6\text{O}_{17}$ : ● for this low-temperature synthetic work and ○ for the high-temperature synthetic work by Ramanujachary et al. [26].

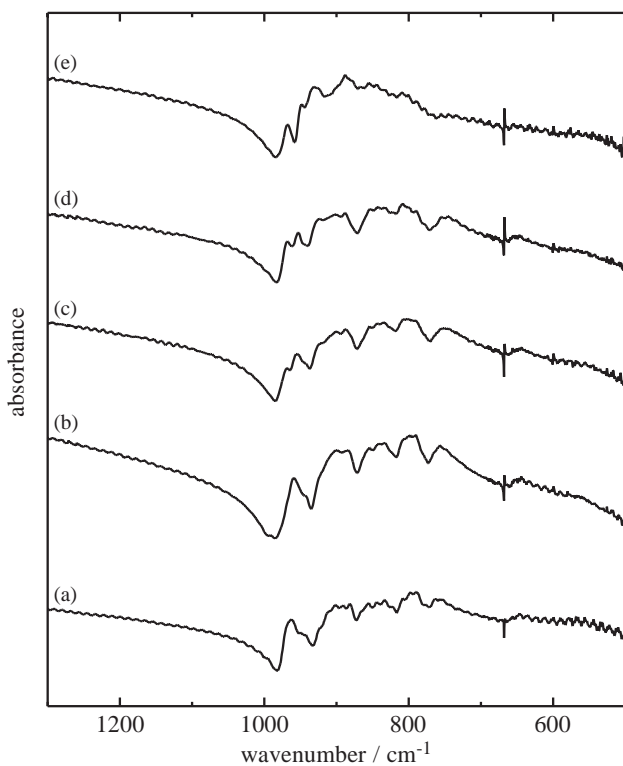


Fig. 8. IR spectra of the products  $(\text{Li}_{1-x}\text{Na}_x)_{0.9}\text{Mo}_6\text{O}_{17}$ :  $x = 0.0$  (a),  $0.31$  (b),  $0.56$  (c),  $0.69$  (d), and  $1.0$  (e).

system at lower temperature, but also an access to structures which are not obtained by usual high-temperature methods.

## 5. Preparation of compounds other than alkali-metal bronzes

As mentioned above, our synthetic route is very suitable for preparation of alkali-metal bronzes at lower temperature. It is expected that our synthetic route is also useful for preparation of compounds other than the bronze. In order to examine the expectation, we tried to prepare molybdenum oxide-based compounds with rare-earth metal cation ( $\text{La}^{3+}$  and  $\text{Gd}^{3+}$ ).

Figs. 9a and 10 show the XRD pattern and the TG-DTA curves of a mixture with Gd content ( $[\text{Gd}]/[\text{Mo}]$ ) of 0.5 and MOSMo of 4.5, which mixture was prepared using gadolinium acetate as a Gd source. The as-prepared mixture was amorphous and released hydration water at ca. 360 K and the acetate moiety at ca. 640 K, respectively, when heated in  $\text{N}_2$  gas. The product heated at 773 K in  $\text{N}_2$  gas remained amorphous (Fig. 9b), and a mixture of  $\text{Gd}_2\text{Mo}_3\text{O}_9$  and  $\text{MoO}_2$  was formed by heating at 1273 K (Fig. 9c). By heating the mixture with La content  $[\text{La}]/[\text{Mo}]$  of 0.5 and MOSMo of 4.5  $\text{La}_2\text{Mo}_3\text{O}_9$  was also obtained together with  $\text{MoO}_2$  and other undefined phases.

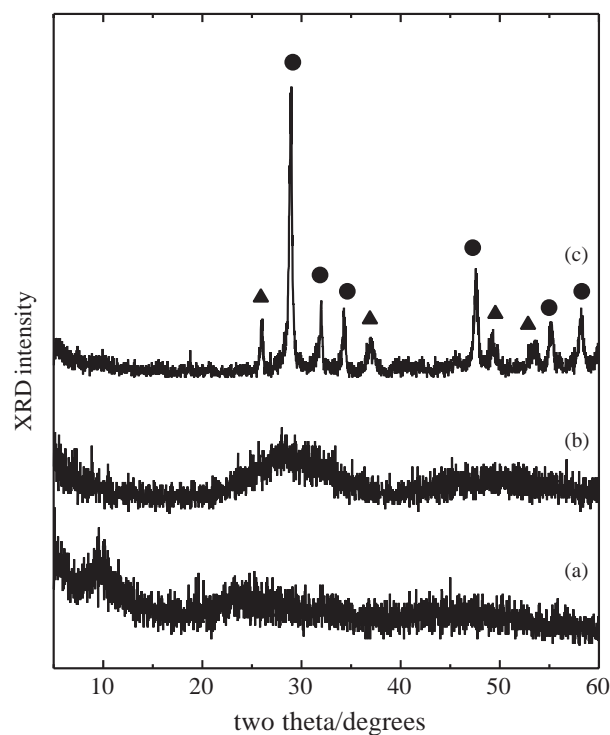


Fig. 9. XRD patterns of the amorphous mixture with Gd content of 0.5 and MOSMo of 4.5 (a), and of its heat-treated products in  $\text{N}_2$  gas at 773 K (b) and at 1273 K (c). Symbols ● and ▲ indicate  $\text{Gd}_2\text{Mo}_3\text{O}_9$  and  $\text{MoO}_2$ , respectively.

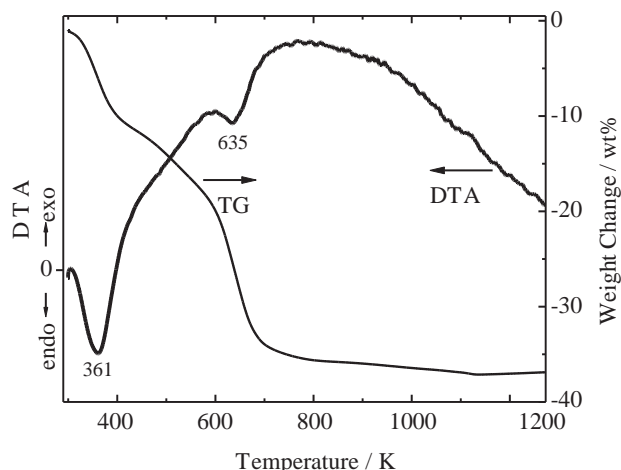


Fig. 10. TG-DTA curves in  $N_2$  gas of the amorphous mixture with Gd content of 0.5 and MOSMo of 4.5.

$Ln_2Mo_3O_9$  ( $Ln$  = rare-earth metal) is paramagnetic with contribution of  $Mo^{4+}$  and is a metastable phase [27–29]. This fact suggests that our synthetic route is effective to enable access to interesting compounds such as metastable phases, even in the cases of compounds other than alkali-metal bronzes.

## 6. Conclusions

By using our low-temperature synthetic route we successfully prepared Cs blue bronze and solid solutions concerning blue and purple bronzes, which have attracted many researchers because of their interesting properties owing to CDW or low-dimensional electronic structure. It was also revealed that our synthetic routes are applicable to compounds other than alkali-metal bronzes, which compounds might not be obtained by usual high-temperature methods.

It should be emphasized that our low-temperature route can provide easy compositional control and open an access to the structures, which cannot be realized by the usual high-temperature methods. At the present moment scope of the application of this low-temperature route is limited to preparation of molybdenum oxide-based compounds. The scope, however, will be spread widely depending on the variety of giant species that will be found in future.

## Acknowledgments

The authors thank Dr. Masao Hashimoto for his valuable discussion.

## References

- [1] J.D. Mackenzie, *J. Non-Cryst. Solids* 73 (1985) 631.
- [2] A. Stein, S.W. Keller, T.E. Mallouk, *Science* 259 (1993) 1558.
- [3] B. Gerand, L. Seguin, *Solid State Ionics* 84 (1996) 199.
- [4] J. Oi, A. Kishimoto, T. Kudo, *J. Solid State Chem.* 103 (1993) 176.
- [5] J. Livage, M. Henry, C. Sanchez, *Prog. Solid State Chem.* 18 (1988) 259.
- [6] C. Tsang, A. Dananjay, J. Kim, A. Manthiram, *Inorg. Chem.* 35 (1996) 504.
- [7] C.F. Tsang, A. Manthiram, *J. Mater. Chem.* 7 (1997) 1003.
- [8] K. Eda, K. Furusawa, F. Hatayama, S. Takagi, N. Sotani, *Bull. Chem. Soc. Jpn.* 64 (1991) 161.
- [9] K. Eda, T. Ito, N. Sotani, *Bull. Chem. Soc. Jpn.* 72 (1999) 2451.
- [10] K. Eda, *Chem. Lett.* (2001) 74.
- [11] A. Müller, J. Meter, E. Krickemeyer, E. Diemann, *Angew. Chem. Int. Ed. Engl.* 35 (1996) 1206.
- [12] B.T. Collins, K.V. Ramanujachary, M. Greenblatt, J.V. Waszczak, *J. Solid State Chem.* 77 (1988) 348.
- [13] K. Eda, T. Miyazaki, F. Hatayama, N. Sotani, *J. Solid State Chem.* 137 (1998) 12.
- [14] J. Dumas, C. Schlenker, J. Marcus, R. Buder, *Phys. Rev. Lett.* 50 (1983) 757.
- [15] M. Greenblatt, W.H. McCarroll, R. Neifeld, M. Croft, J.V. Waszczak, *Solid State Commun.* 51 (1987) 671.
- [16] M. Greenblatt, *Chem. Rev.* 88 (1988) 31.
- [17] J. Choi, J.L. Musfeldt, J. He, R. Jin, J.R. Thompson, D. Mandrus, X.N. Lin, V.A. Bondarenko, J.W. Brill, *Phys. Rev. B* 69 (2004) 085120.
- [18] J. Choi, J.D. Woodward, J.L. Musfeldt, X. Wei, M.-H. Whangbo, J. He, R. Jin, D. Mandrus, *Phys. Rev. B* 70 (2004) 085107.
- [19] K. Eda, Y. Sato, Y. Iriki, *Chem. Lett.* (2002) 952.
- [20] F. Izumi, T. Ikeda, *Mater. Sci. Forum* 321–324 (2000) 198.
- [21] C. Choain, F. Marion, *Bull. Soc. Chim. Fr.* (1963) 212.
- [22] L.E. Depero, M. Zocchi, F. Zocchi, F. Demartin, *J. Solid State Chem.* 104 (1993) 209.
- [23] J. Graham, A.D. Wadsley, *Acta Crystallogr.* 20 (1966) 93.
- [24] M. Onoda, K. Toriumi, Y. Matsuda, M. Sato, *J. Solid State Chem.* 66 (1987) 163.
- [25] M. Onoda, Y. Matsuda, M. Sato, *J. Solid State Chem.* 69 (1987) 67.
- [26] K.V. Ramanujachary, B.T. Collins, M. Greenblatt, P. McNally, W.H. McCarroll, *Solid State Ionics* 22 (1986) 105.
- [27] J. Jagannatha, A. Manthiram, *J. Chem. Soc. Dalton* (1981) 668.
- [28] E.A. Tkachenko, P.P. Fedorov, *Inorg. Mater.* 39 (Suppl. 1) (2003) S25.
- [29] H. Prevost-Czeskleba, G. Tourne, *Proceedings of the 15th Rare Earths Research Conference, Rolla, 1981*, p. 271.